

Examples of spatial and temporal variations of some fine-grained suspended particle characteristics in two Danish coastal water bodies

Variations spatiales et temporelles des matières fines en suspension dans deux masses d'eau des côtes danoises

Ole Aarup Mikkelsen *

Bedford Institute of Oceanography, Habitat Ecology Section, PO Box 1006, Dartmouth, NS B2Y 4A2, Canada

Received 5 June 2001; received in revised form 18 October 2001; accepted 22 October 2001

Abstract

In June and September of 1999, a LISST-100 in situ laser diffraction particle sizer was used to analyse the temporal and spatial variation of the beam attenuation coefficient, the in situ median particle (aggregate) diameter and the median volume concentration of suspended matter in two Danish coastal water bodies. One of the study sites was generally exposed to wind, while the other was quite sheltered. Measurements of the mass concentration of total suspended matter and chl *a* were made simultaneously. The in situ median effective density, settling velocity and vertical flux of the suspended matter are computed. Results demonstrate that in September, the in situ median aggregate diameter, settling velocity and vertical flux was smaller (by a factor of up to 16) and the concentration higher (by a factor of up to almost two) than in June. This is attributed to varying degrees of turbulence in the water in the weeks preceding the field work, causing aggregates to break up (lowering in situ aggregate diameter and settling velocity) and sediment to be resuspended (increasing concentration) in September. The fractal dimension of the suspended aggregates is estimated. The fractal dimension is found to increase from June to September at both study sites, supporting the notion of aggregate break-up in September due to turbulence in the upper part of the water column. An algae bloom occurred at the sheltered study site in September. In situ particle size spectra from this site demonstrated increasing aggregate sizes towards the bottom. It is suggested, that the increase in size is due to biologically induced aggregation, causing large aggregates to settle out of the upper part of the water column, leaving finer particles and aggregates behind. © 2002 Ifremer/CNRS/IRD/Éditions scientifiques et médicales Elsevier SAS. All rights reserved.

Résumé

En juin et en septembre 1999, un compteur de particules à diffraction laser (LISST-100) a permis d'analyser les variations du coefficient d'extinction, du diamètre moyen des particules et du volume moyen de la matière en suspension dans deux masses d'eau des côtes danoises. Un des sites d'études était exposé au vent alors que le second était plutôt abrité. Le poids des particules en suspension et la teneur en chlorophylle *a* ont été mesurés. Les résultats montrent qu'en septembre, le diamètre moyen des agrégats in situ, la vitesse de sédimentation et le flux vertical sont plus faibles (par un facteur qui peut atteindre 16) et les concentrations plus fortes (par un facteur qui peut atteindre 2) qu'en juin. Ceci est attribué à la turbulence dans les semaines précédant les mesures, ce qui entraîne une rupture des agrégats, abaissant leur diamètre et leur vitesse de sédimentation. Cela conduit également à une resuspension du sédiment, d'où une élévation de la concentration en septembre. La dimension fractale des agrégats est estimée. Elle s'élève de juin à septembre aux deux sites, ce qui renforce l'hypothèse d'une rupture des agrégats en septembre, liée à la turbulence dans la couche superficielle. Une floraison algale se développe, au site abrité, en septembre. Le spectre de taille de particules in situ à ce site montre un accroissement de la taille des agrégats vers le fond. Cet accroissement en taille serait dû à une agrégation biologique entraînant la sédimentation de larges agrégats, la couche superficielle conservant seulement les particules et les agrégats fins. © 2002 Ifremer/CNRS/IRD/Éditions scientifiques et médicales Elsevier SAS. Tous droits réservés.

* Corresponding author.

E-mail address: MikkelsenO@mar.dfo-mpc.gc.ca (O.A. Mikkelsen).

Keywords: Aggregation; Laser diffraction; Particle size spectra; Fractal dimension; Settling velocity

Mots clés: Agrégation; Diffraction laser; Spectre de taille des particules; Dimension fractale; Vitesse de sédimentation

1. Introduction

The spatial variation of, for example, the variation in the concentration of total suspended matter (*TSM*) in near-coastal areas or estuaries can be quite difficult to describe, due to the effect of tides, coastal currents and waves. From a sedimentological and a physical point of view also the spatial variation in other parameters relating to the behaviour and state of suspended matter is of interest, for example the in situ particle size, density and settling velocity (all prone to rapid change due to particle aggregation). Remote sensing can to some degree be used to study some parameters (but definitely not all), for example *TSM* (Ritchie and Cooper, 1988; Stumpf and Goldschmidt, 1992; Robinson et al., 1998). However, it has been shown that it is not possible to produce a remote sensing algorithm for this purpose that has general validity, due to the profound influence on reflectance of changes in the in situ particle size and density (Bale et al., 1994; Mikkelsen, 2001). Therefore, the only feasible way to obtain knowledge of the spatial variation in *TSM* and other parameters of interest, for example in situ aggregate size or settling velocity, is by sampling from a vessel.

Synoptic or semi-synoptic maps showing the spatial variation of *TSM* and other parameters related to the suspended matter, for example settling velocity, would be very useful for sedimentological and environmentally related studies, as well as for monitoring purposes. So far, however, these parameters are to the knowledge of this author not incorporated in any monitoring program. Such maps would have to be produced by making in situ measurements from a vessel cruising the study area.

Several researchers have presented results from coastal areas where it has been assumed that the variation in, for example, *TSM*, in situ particle (aggregate) size or aggregate density is time invariant (Baban, 1993, 1997; Holdaway et al., 1999; Forget et al., 1999). This paper aims at demonstrating that this is hardly the case and that especially in situ aggregate size may vary almost one order of magnitude in a relatively confined area. Thus, this paper sets out to investigate and describe the spatial and temporal variation of a number of parameters related to suspended matter in two Danish coastal waters. The parameters in question (*TSM*, beam attenuation, in situ aggregate size, in situ aggregate surface area, in situ density, in situ settling velocity, in situ settling flux, and chl *a*) are only rarely assessed simultaneously, even less so is their spatial and temporal variation investigated.

2. Material and methods

2.1. Study sites

Field work was carried out in a near-coastal body of water in the Eastern North Sea, 3–18 km off the coast of the barrier island Fanø on the Danish west coast and in the Horsens Fjord, a sheltered fjord system at the east coast of the Jutland peninsula (Fig. 1, 2).

The North Sea (NS) study site (Fig. 1) is micro-tidal with a semi-diurnal, tidal range of 1.5–1.8 m. Along the eastern-most edge of the study area, the water depth is around 4 m

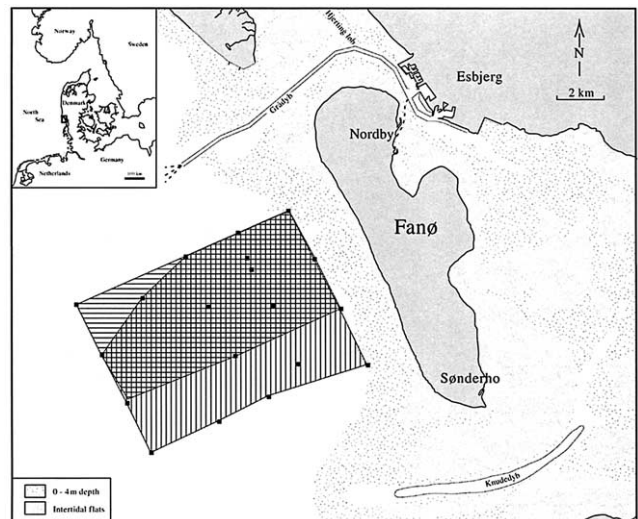


Fig. 1. The study site in the North Sea, off the west coast of the barrier island Fanø. The area hatched with horizontal lines was covered on 14 June, while the area hatched with vertical lines was covered on 11 September. Dots show sampling stations (see also Fig. 3).

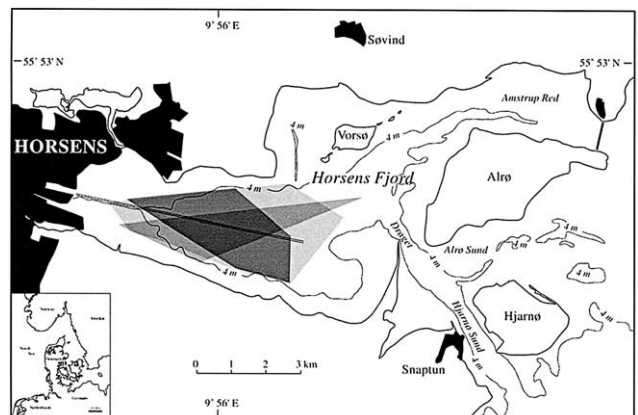


Fig. 2. The study area in the Horsens Fjord on the east coast of the Jutland peninsula. The areas delimited by the three shades of grey (from light to dark) indicate the areas investigated at 15 June, 6 September, and 13 June, respectively (see also Fig. 4).

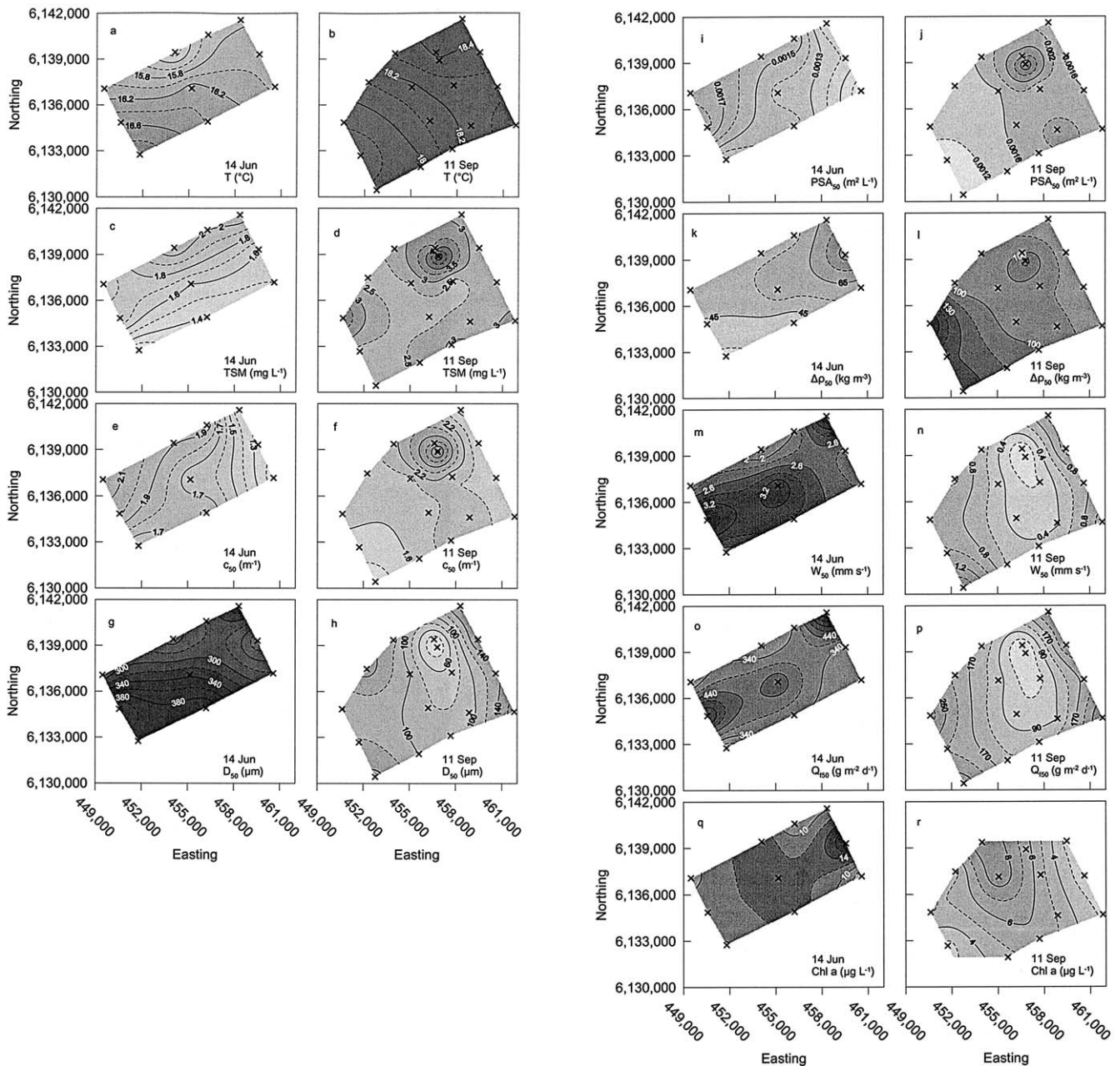


Fig. 3. The variation in June and September at the North Sea study site of the temperature (T), total suspended matter concentration (TSM), median beam attenuation coefficient (c_{50}), median particle size (D_{50}), median projected surface area (PSA_{50}), median effective density ($\Delta\rho_{50}$), median settling velocity (W_{50}), median vertical flux (Q_{50}), and chl a . Darker colours show higher values.

at low tide and along the westernmost edge about 16 m. The easternmost edge of the area runs parallel to the shore of the barrier island Fanø, at a distance of 2 km off the shore. The study area lies more or less between two tidal inlets connecting the Wadden Sea with the North Sea: to the north the tidal inlet Grådyb, and to the south the tidal inlet Knudedyb. The area is very exposed to winds from westerly directions and is only in a relatively sheltered position when the wind is from the east. The major resuspension agent is wave activity related to windy periods. Waters in the area are generally well mixed. The NS site can furthermore be considered a transition zone between the Wadden sea area

and the North Sea per se, and is generally not well investigated, compared to these two areas.

The Horsens Fjord (HF) (Fig. 2) is also micro-tidal, but with a tidal range of ca. 0.6 m. In general, noticeable water fluctuations in the HF are due to meteorological conditions, not the regular astronomical tide. A halocline with a salinity difference of up to 4–5 is usually present in most of the fjord. For winds from west, north or south, the fetch is only a few kilometres. Only for winds from the east is there a significant wave activity, causing resuspension of bottom sediments and mixing of the stratified water column. Mud or sandy mud constitutes the bottom sediments.

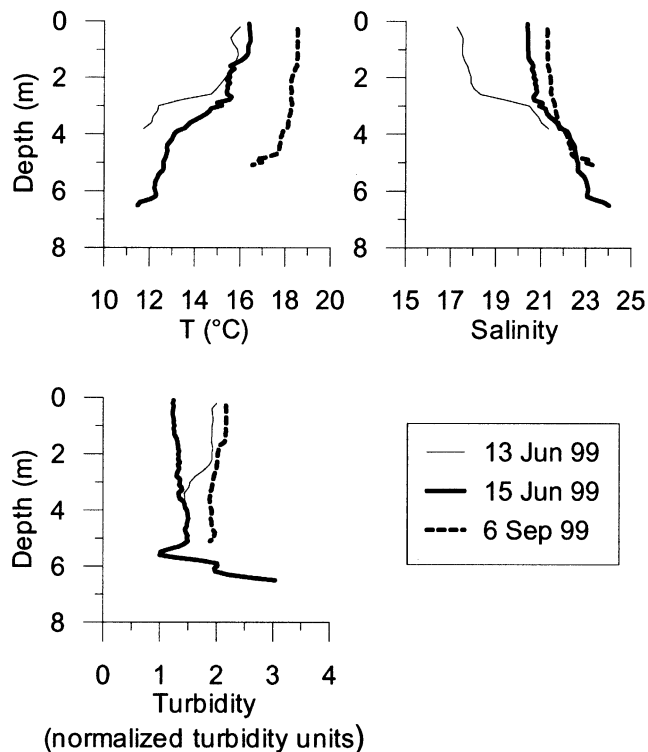


Fig. 4. Examples of CTD measurements of temperature, salinity and normalised turbidity from the Horsens Fjord. Turbidity is normalised to the lowest measured level of turbidity on the three dates. The measurements were all carried out at a station in the middle of the area covered on all three field work dates (cf. Fig. 2).

2.2. Methods

2.2.1. Sampling scheme

Particle measurements – Fieldwork was carried out during five days in 1999 at a number of stations. In the NS on 14 June (10 stations) and 11 September (17 stations) and in the HF on 13 June (7 stations), 15 June (11 stations) and 6 September (8 stations). At each station, the particle size spectrum (*PSS*), the volume concentration (*VC*), the beam attenuation coefficient (*c*) and the water temperature was measured in situ one meter below the surface (mbs). Measurements were carried out using an LISST-100 type C laser diffraction particle sizer (Agrawal and Pottsmith, 2000), measuring particle volume in 32 logarithmically spaced size classes in the range 2.5–500 μm . Raw data were sampled at 4 Hz, whereupon average values for five measurements were computed and recorded on the on-board data logger. All stored raw data were thus averaged over a period of 1.25 s. Upon retrieval of the instrument, the raw data were off-loaded and analysed by means of the LISST data processing programme version 3.22, thus yielding the particle size spectrum (*PSS*), volume concentration (*VC*), beam attenuation coefficient (*c*) and the temperature (for details, cf. Agrawal and Pottsmith, 2000). Note that due to the short time it took for the LISST to write data to the data logger, there is a 1.67 s period, not 1.25 s, between each data set consisting of a *PSS*, *VC*, *c*, and temperature. The

median diameter was derived from each *PSS*. For each station the processed data were grouped into one min intervals, i.e. 36 data sets min^{-1} . Finally, median values for diameter (D_{50}), *VC* (VC_{50}), and *c* (c_{50}), were found for each one min interval.

Water sampling – Water samples were taken with a 2 L water sampler at the same depth and time as the LISST measurements. *TSM* was determined by filtering the water samples through pre-filtered, pre-weighed Millipore filters type HA (nominal retention diameter 0.45 μm). The filters were flushed three times with de-ionized water (in order to remove excess salt) and oven dried for 1.5 h at 65 $^{\circ}\text{C}$. Subsequently the filters were allowed to adjust to room temperature for 0.5 h and weighed with an accuracy of ± 0.1 mg. Pre-weighed blanks followed the same procedure in order to determine whether or not the filters themselves gained or lost weight during the filtration work. *Chl a* was determined by HPLC from water samples filtered on Whatman GF/F filters.

CTD measurements – In the HF a CTD probe (SeaBird SBE 25) was used for obtaining information regarding thermo- and haloclines, while a Kent Temperature Salinity Bridge type MC5 was used in the North Sea.

2.2.2. Weather conditions

On all fieldwork days the weather was much alike. The wind was light, and wave heights were below 0.1–0.5 m at the NS site (lowest in June) and below 0.1–0.2 m in the HF. However, the weather had been quite different in the weeks preceding the June and September study periods. In June, a prolonged period of calm and quiet weather with wave heights generally below 0.4 m persisted in the week up to the 13–15 June. Contrary, in the week before 6–11 September a prolonged period with strong westerly winds and wave heights up to 2 m (in the NS) persisted. Therefore, with respect to wind- and wave-induced energy in the water column, the conditions in the NS were much different from June to September whereas in the HF they were more or less the same, due to the limited fetch in the HF.

In the NS, fieldwork on 14 June began 1.5 h after low water and had duration of 5.5 h. On 11 September, fieldwork began 45 min before low water and had duration of 4.25 h. Thus, at the NS site, fieldwork was carried out mainly in the flood period on both study dates. In the HF, fieldwork began less than 2 h before high water and had duration of 6–8 h at all study dates. Therefore, at all study dates in the HF fieldwork were mainly carried out in the ebbing period.

2.2.3. Calculations

From the measurements of *TSM* and VC_{50} , the median effective density, $\Delta\rho_{50}$ and the median settling velocity, W_{50} of the suspended particles was calculated using equations 1–2 (cf. Mikkelsen and Pejrup 2000, 2001):

$$\Delta\rho_{50} \approx \frac{TSM}{VC_{50}} \quad (1)$$

Table 1
Area-averaged median values of the investigated parameters, together with their range of variation

Date Parameter	The NS, 14 Jun 99	The NS, 11 Sep 99	The HF, 13 Jun 99	The HF, 15 Jun 99	The HF, 6 Sep 99
T (°C)	16.1	18.1	15.7	15.9	18.4
	15.1–17.0	17.8–18.5	14.8–16.6	15.0–16.6	17.7–18.9
TSM (mg l ⁻¹)	1.7	2.8	2.2	2.0	2.7
	1.2–2.1	2.0–5.5	1.7–2.3	1.4–3.4	1.8–3.6
c_{50} (m ⁻¹)	1.73	1.85	4.42	3.15	3.48
	1.13–2.20	1.11–3.85	3.08–5.42	2.24–3.89	2.83–5.34
D_{50} (µm)	322	117	142	164	23
	221–425	21–173	95–282	97–251	17–31
PSA_{50} (×10 ⁻⁴ m ² l ⁻¹)	14.3	16.5	37.4	26.2	26.7
	9.2–18.4	8.6–36.6	25.9–47.7	17.9–33.1	17.0–44.9
ΔQ_{50} (kg m ⁻³)	52	98	31	38	130
	33–90	72–178	22–38	19–103	107–174
W_{50} (mm s ⁻¹)	2.57	0.74	0.32	0.48	0.03
	1.54–3.94	0.03–1.60	0.14–0.98	0.23–1.34	0.02–0.10
Q_{f50} (g m ⁻² d ⁻¹)	366	171	60	90	8
	247–700	11–309	25–186	37–334	4–17
Chl a (µg l ⁻¹)	11.4	5.1	–	1.7	7.2
	6.3–18.6	2.3–8.9	1.1–2.2	0.8–3.1	4.1–14.6
Area covered (km ²)	48.7	67.5	5.5	9.6	4
No. of stations	10	17	7	11	8
D_f	2.37	2.67	0.34	0.19	2.47

T , temperature; TSM , total suspended matter concentration; c_{50} , median beam attenuation coefficient; D_{50} , median particle (aggregate) diameter; PSA_{50} , median projected surface area; ΔQ_{50} , median effective density; W_{50} , median settling velocity; Q_{f50} , median vertical flux; D_f , the fractal dimension of the suspended aggregates; chl a , chlorophyll a concentration.

and

$$W_{50} = \frac{D_{50}^2 \cdot \Delta \rho_{50} \cdot g}{18 \cdot \eta} \quad (2)$$

Equation 2 is Stokes's Law, where g is gravitational acceleration and η is water viscosity.

It should be noted that the W_{50} computed from (2) may not necessarily be the actual W_{50} , rather the potential W_{50} . The actual W_{50} could be lower than the potential W_{50} , for example due to turbulence in the water column. Also, it must be recognised that Stokes's Law should only be used for values of Reynold's number (Re) < 1. However, it was shown by Sternberg et al. (1999) that inclusion of large aggregates (diameter up to 760 µm) with $Re > 1$ made no apparent change to their observed relationship between aggregate settling velocity and diameter. In this study, the largest D_{50} was found to 425 µm (cf. Table 1), suggesting that the use of Stokes's Law for computation of W_{50} is suitable.

The projected surface area (Bale et al., 1994) of the suspended particles is given according to equation 3 (for details, cf. Mikkelsen, 2001):

$$PSA_{50} = \sum_{i=1}^{32} 1.5 \cdot \frac{VC_i}{x_i} \quad (3)$$

where x_i is the midpoint of size class i and VC_i is the volume concentration in size class i . Again, a PSA was calculated for each size spectrum, and the median value (PSA_{50}) derived for each data set. The PSA can be considered a proxy for remotely sensed water leaving reflectance (Bale et al., 1994; Mikkelsen, 2001). Therefore, it is important to

gain knowledge regarding the potential variation in this parameter.

Finally, a potential vertical median flux, Q_{f50} , of the suspended matter can be computed according to equation 4:

$$Q_{f50} = W_{50} \cdot TSM \quad (4)$$

3. Results and discussion

The spatial and temporal variation of the parameters temperature (°C), TSM (mg l⁻¹), c_{50} (m⁻¹), D_{50} (µm), PSA_{50} (m² l⁻¹), ΔQ_{50} (kg m⁻³), W_{50} (mm s⁻¹), Q_{f50} (g m⁻² d⁻¹), and chl a (µg l⁻¹) was mapped for the NS site (Fig. 3a, r) and for the HF (Fig. 5a, z). The median values used for plotting Fig. 3 and 5 are from the same minute where water sampling took place. For each area, the nine parameters were weighted over the entire area in order to find a mean value for each parameter. These are summarized in Table 1. Note that on 13 Jun, the spatial coverage of the chl a sampling was less adequate than for the other parameters, hence it is not mapped for this date in Fig. 5.

First, the seasonal variation within each of the study areas is considered. Second, the variation between the NS site and the HF in June and September, respectively, is considered.

3.1. Variation at the NS site

From Table 1 and Fig. 3a, b, the water temperature at the NS study site is seen to have risen by approximately 2 °C from June to September. Table 1 and Fig. 3c, d demonstrate

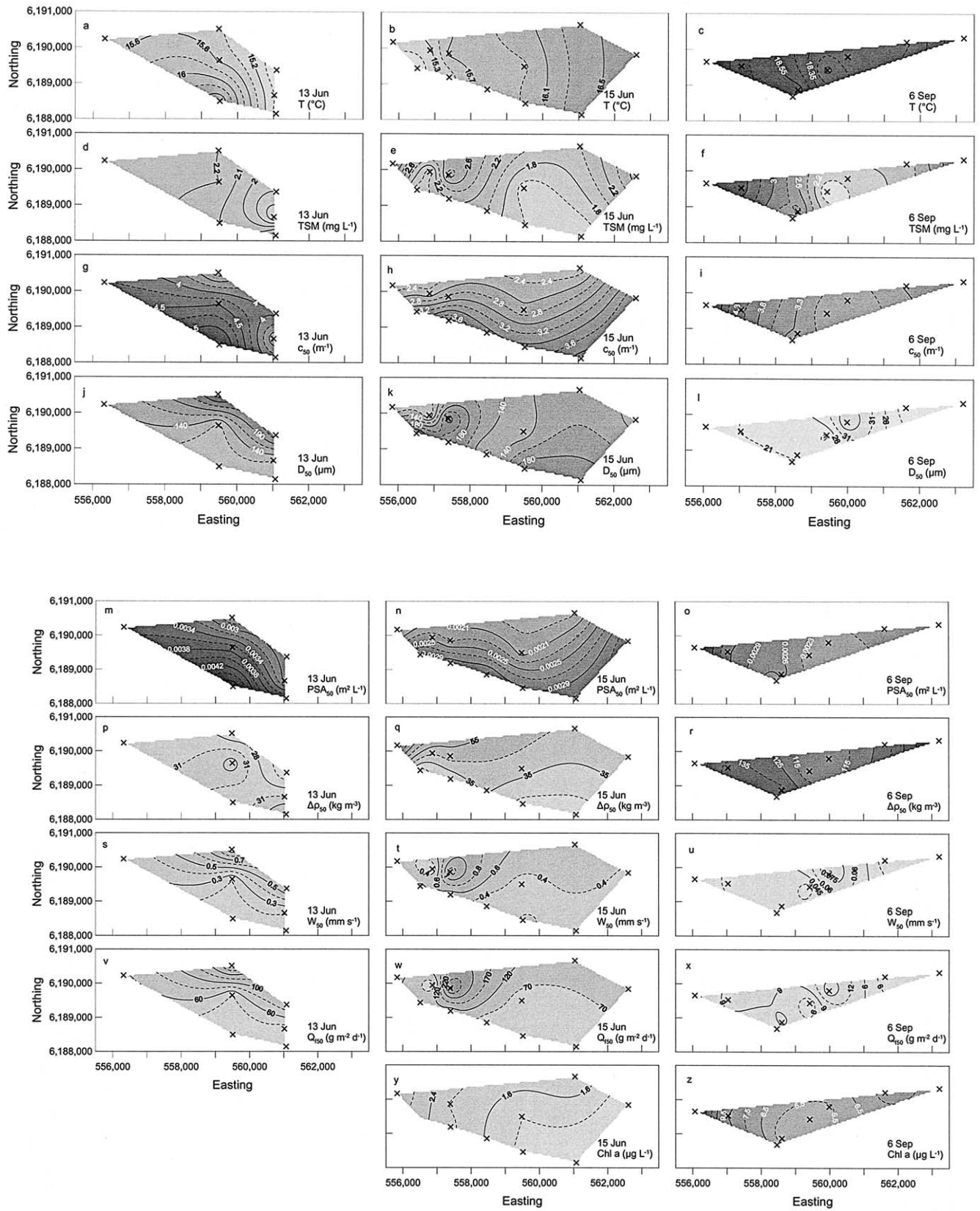


Fig. 5. The variation in June and September in the Horsens Fjord of the temperature (T), total suspended matter concentration (TSM), median beam attenuation coefficient (c_{50}), median particle size (D_{50}), median projected surface area (PSA_{50}), median effective density ($\Delta\rho_{50}$), median settling velocity (W_{50}), median vertical flux (Q_{150}), and chl a . Darker colours show higher values.

that *TSM* has almost doubled; from 1.7 to 2.8 mg l⁻¹ on average, probably related to the windy conditions prior to the September field work. In June there is an increase in *TSM* when going towards the northwest, while in September there is no clear trend in the distribution of *TSM*. However, c_{50} (Fig. 3e, f) is almost constant (~1.8 m⁻¹) for the two dates. Also the spatial variation in c_{50} differs from that of *TSM*: in June, c_{50} almost doubles towards the west, while in September it is quite constant (~1.6–1.9 m⁻¹) over a large part of the area. The constant value for c_{50} is due to the fact that PSA_{50} is almost constant (Table 1, Fig. 3 i, j). c_{50} is, in reality, dependent on the PSA_{50} and will only vary linearly with mass concentration if the in situ particle size and density are constant (Mikkelsen, 2001). The constant value for c thus demonstrates that a change in the in situ size and/or density of the suspended matter has occurred (cf. Mikkelsen, 2001). This is confirmed when considering the change in D_{50} and ΔQ_{50} between the two dates: D_{50} is reduced to approximately a third between June and September, while ΔQ_{50} has almost doubled (Table 1). D_{50} is quite constant in June, varying approximately a factor of two throughout the area, increasing towards the south west (Fig. 3 g). However, in September D_{50} varies more than a factor of eight, with a minimum in the northern part and increasing towards the east and west (Fig. 3h). W_{50} is seen to be almost four times higher in June than September (Fig. 3m, n, Table 1), due to the larger value for D_{50} in June. There is a slight tendency for W_{50} to increase towards the west in June, whereas the same pattern as for D_{50} is observed in September. Also, due to the larger variation in D_{50} in September than in June, W_{50} varies more in September. As Q_{f50} is mainly related to W_{50} , and to a lesser degree *TSM*, the temporal and spatial variation in Q_{f50} resembles that of W_{50} (Fig. 3o, p). Finally, chl *a* is seen to be quite uniformly distributed in June (Fig. 3q), whereas in September chl *a* decreases from the centre of the area towards the west and east (Fig. 3 r). Chl *a* is almost halved from June to September (Table 1).

3.2. Variation in the HF

First, a CTD profile obtained in the centre of the area covered at all three study dates is considered (Fig. 4).

The thermo- and halocline mentioned above is clearly seen. The maximum temperature difference on the three dates is 5 °C (15 Jun 1999) and the maximum salinity difference is 4.1 (13 Jun 1999). The turbidity measurements reveal that by September turbidity had increased by up to a factor of 2, compared to June. On 15 June, a pronounced increase in turbidity appears close to the bottom. Current measurements were carried out in the fjord on several occasions during an earlier field campaign. These measurements showed that the current velocity 100 cm above the bottom, u_{100} , rarely exceeded 0.05–0.10 m s⁻¹. Such low values of u_{100} are usually not capable of creating a shear stress strong enough to resuspend sediment. This is espe-

cially so in an environment where the bottom sediment is composed mainly of mud. Andersen (1999) showed that for mudflats in the Danish Wadden Sea the regular current with a maximum mean velocity of 0.15–0.20 m s⁻¹ was not capable of resuspending sediment. Only during windy events could the shear stress created by wind-induced waves cause resuspension.

TSM is quite constant around 2 mg l⁻¹ on 13 and 15 June, but with a larger variation on 15 June (Table 1). There is a tendency for increasing *TSM* towards the head of the fjord on 13 June, but this is less clear on 15 June (Fig. 5d, e). c_{50} has decreased 30% from 13 June to 15 June (Table 1), which is consistent with a decrease in PSA_{50} , related to a slight increase in D_{50} (Table 1 and Fig. 5g, h). ΔQ_{50} , W_{50} , and Q_{f50} for 13 and 15 June are all comparable in magnitude (Table 1). With respect to the spatial variation on 13 and 15 June, it is seen that c_{50} and PSA_{50} decrease towards the northern side of the fjord on both dates (Fig. 5g, h, 5m, n). ΔQ_{50} is almost constant throughout the fjord on 13 June (Fig. 5p), whereas there is a tendency to an increase towards the west on 15 June (Fig. 5q). W_{50} and Q_{f50} increase towards the north side of the fjord on 13 June, but on 15 June there is a slight susceptibility to an increase towards the west (Fig. 5s, t, 5v, w), coincident with the spatial variation in D_{50} and ΔQ_{50} . Chl *a* clearly increases towards the head of the fjord (west) on 15 June (Fig. 5y). Chl *a* concentrations on 13 and 15 June are of similar magnitude (Table 1).

In September, *TSM* has increased (Table 1). c_{50} though, is almost equal to the 15 June values, as is PSA_{50} . This is related to a drastic increase in ΔQ_{50} from June to September, which combined with a concurrent decrease in D_{50} serves to keep PSA_{50} constant. Compared to the values of 15 June, W_{50} and Q_{f50} has been reduced by approximately 90%, due to the decrease in D_{50} . *TSM*, C_{50} , PSA_{50} and ΔQ_{50} now all increase towards the west (Fig. 5f, i, o, r), while no clear tendency exist for D_{50} , W_{50} or Q_{f50} (Fig. 5l, u, x). Chl *a* has increased by more than a factor of three from June to September, with a tendency to a minimum (~5.5 µg l⁻¹) in the centre of the September study area, and increasing towards the west and east. This is in accordance with observations from fjords nearby, where algae blooms were abundant in September of 1999. The increase in *TSM* could be related to the increase in chl *a*, as resuspension of bottom sediments is not very likely to have occurred (cf. discussion above).

So, over a short (order of a few days) time scale, and provided that the weather conditions are alike, there seems to be indications that the magnitude of the investigated parameters in the HF does not change to any large degree (Table 1). However, their spatial distribution may well have changed, as demonstrated on Fig. 5d, e, 5j, k, 5p, q, 5v, w.

3.3. Variation between the NS and HF in June

From Fig. 3 and 5 and Table 1, it appears that *TSM* is slightly lower in the NS than in the HF (~20%). However,

c_{50} is 45–60% lower in the NS than in the HF. As before, this is related to the difference in PSA_{50} between the two areas. The reason for the much smaller value for PSA_{50} in the NS is the larger aggregates there, D_{50} at the NS site being more than a factor of two larger than in the HF. The reason for this is not clear, but it could be related to different algae species and/or algae concentrations at the two dates. From the difference in ΔQ_{50} it is seen that the aggregates in the NS are more tightly packed, this could indicate a larger proportion of mineral grains in the NS aggregates. Finally, as W_{50} is computed from the D_{50} , these values are also larger for the NS than for the HF, between a factor of 4.4 and 7 compared to the HF. Likewise, Q_{f50} is a factor of 3.7 to 5 larger in the NS. Hence, there seems to be larger potential for mass settling at the NS site than in the HF. However, it must be remembered that the Q_{f50} is a potential flux only. A large part of the suspended matter in the water column at the study date could have been resuspended matter from within the area, hence giving a false impression of the flux. Chl *a* is almost a factor of five higher at the NS study site than in the HF. This could be related to advection of Wadden Sea water, which is known to have a high concentration of chl *a* due to favourable conditions of growth in the Wadden Sea area.

3.4. Variation between the NS and HF in September

From Fig. 3 and 5 and Table 1, it is seen that values for TSM are now the same in the two areas, though the range of variation is slightly larger at the NS site than in the HF. c_{50} is still higher in the HF than in the NS. As for June, this is related to the difference in PSA_{50} , controlled by the difference in D_{50} and ΔQ_{50} . The aggregates in the HF are now the more tightly packed, indicating inclusion of mineral grains (perhaps due to resuspension) and/or restructuring of the aggregates due to shear. Most notable is the difference in W_{50} and Q_{f50} . Compared to June, values have decreased in both areas, but most dramatically in the HF. As for June, there seems to be larger potential for mass settling at the NS site than in the HF. Chl *a* is now slightly higher in the HF than at the NS site (due to the bloom in HF), compared to the situation in June.

3.5. Overall variation

The increase in TSM and the concurrent decrease in D_{50} and W_{50} in both areas from June to September could be related to the different meteorological conditions. The windy period in September could easily have caused resuspension of bottom sediments and aggregate break-up, especially at the NS site. As the HF is much more sheltered from the westerly winds, resuspension is probably not the cause for the observed changes in TSM , D_{50} and W_{50} .

Mikkelsen and Pejrup (2001) derived the fractal dimension (D_f) for aggregates at the NS and the HF sites in June and September. An increase in the fractal dimension can

occur if the aggregate is restructured to a more compact one, for example due to shear (Kranenburg, 1994; Risović, 1998). D_f can be derived from a log-log plot of aggregate effective density vs. aggregate size (cf. van der Lee, 2000). Mikkelsen and Pejrup (2001) used samples from throughout the water column (not only from 1 mbs, as in this study) for their estimates of D_f . They reported that D_f in the HF was the same in June and September (~2.3), whereas it increased from 2.1 in June to 2.7 in September at the NS site. Therefore, Mikkelsen and Pejrup (2001) suggested that the reason for the increase in the D_f at the NS site was due to the fact that this area was more exposed than the HF. Thus, the stable value for the fractal dimension in the HF suggested that no restructuring had taken place in the HF.

In this study, D_f was derived for all five study dates, but only for samples taken at 1 mbs (Table 1). It appears that when using the samples from 1 mbs only, the D_f now increases from June to September for both the NS and the HF study sites. It would seem that the values for D_f presented here somewhat contradicts the findings of Mikkelsen and Pejrup (2001). However, as the D_f values presented here (Table 1) are all related to aggregates at 1 mbs, i.e. the upper part of the water column only, the argument that restructuring has taken place might still be valid. While the HF is well sheltered from westerly winds, some turbulence due to wind stress at the surface is still induced in the upper part of the water column, while the lower layers are largely unaffected.

As mentioned earlier, a very windy period persisted in the week before the September field work in both the HF and the NS. In the HF, the westerly wind thus would only induce some turbulence close to the surface, causing aggregates to break up and become restructured into more compact entities, thus increasing D_f in September as observed. The wind induced turbulence could thus explain the decrease in D_{50} in both the HF and at the NS site. However, for the HF another explanation is also possible. The change in D_{50} in the HF could be related to biological processes, such as increased amounts of biogenic exudates. These exudates cause the particles to aggregate and settle out of the upper water column, leaving finer particles and aggregates behind (Avnimelech et al., 1982; Eisma, 1986; Passow et al., 2001). Some evidence for this was found in the particle size spectra from the upper and lower parts of the water column on the stations investigated in September (Fig. 6).

Fig. 6a, b are spectra from 1 mbs at two stations in the HF during the September investigation, while Fig. 6c, d are spectra from 0.5 m above the bottom (mab) at the same stations. D_{50} for the spectra from 1 mbs is ~18 μm , while it is 89 μm and 366 μm for the spectra from 0.5 mab. It is evident that the aggregates are much larger at 0.5 mab than at 1 mbs, between a factor of 4 and 20 for the spectra shown here. This could be related to the settling of larger aggregates from the surface due to biologically induced aggregation. It has been suggested (Avnimelech et al., 1982; Mari

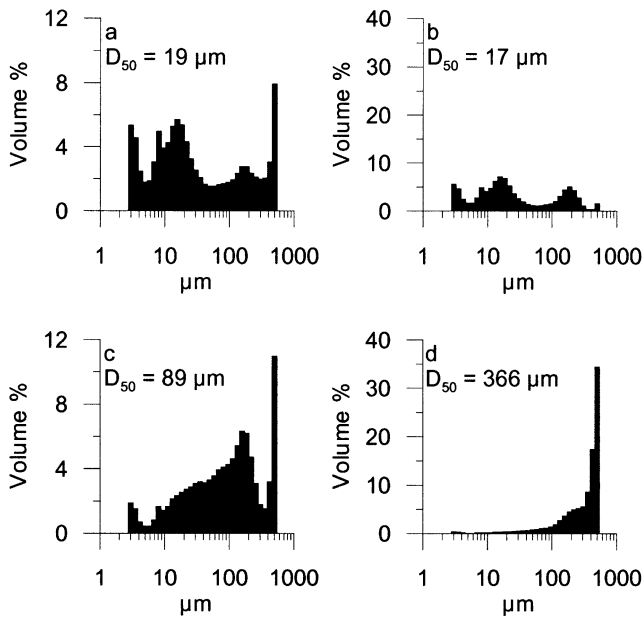


Fig. 6. Examples of variation in particle size spectra at two stations in the Horsens Fjord, 6 September. A, b) size spectra from 1 mbs; c, d) size spectra from 0.5 mab (at the same stations as in a, b). Clearly, a change in the size spectra towards the coarser grain-sizes is obvious when moving from the upper part of the water column towards the bed.

and Kjørboe, 1996) that by the end of algae blooms large aggregates tend to form, rapidly removing dying algal cells from the surface waters. Chl *a* in the HF was more than a factor of three larger in September than in June (Table 1). Therefore, there seems to be some basis for suggesting that biologically induced aggregation in the HF caused aggregation, subsequent settling of the large aggregates into the bottom layer, leaving small particles and aggregates in the upper part of the water column, as demonstrated in Fig. 6a, d.

It should be noted that several of the size spectra in Fig. 6a, d exhibit a rising 'tail' that is eventually cut off at 500 µm, the upper limit of sizes detected by the LISST-100. In fact, this phenomenon was commonly observed in most of the LISST measurements and it indicates the presence of particles larger than 500 µm (cf. Agrawal and Pottsmith, 2000). The influence of particles outside the measurement range on the D_{50} is minimal, however. This can be illustrated by Fig. 7, which shows a size analysis of a sediment sample carried out in the laboratory using a Malvern MasterSizer/E laser. The MasterSizer/E can measure particle sizes in three size ranges; 0.1–80 µm, 0.5–180 µm and 1.2–600 µm by changing the optical configuration of the laser.

Fig. 7a shows a sediment sample analysed using the 0.5–180 µm configuration. A rising tail at the coarse end of the size spectrum appears. Using the 1.2–600 µm configuration for analysis of the same sample yields the result presented in Fig. 7b. No rising tail appears. It is seen from Fig. 7b that only 4.4% of the entire sample is coarser than

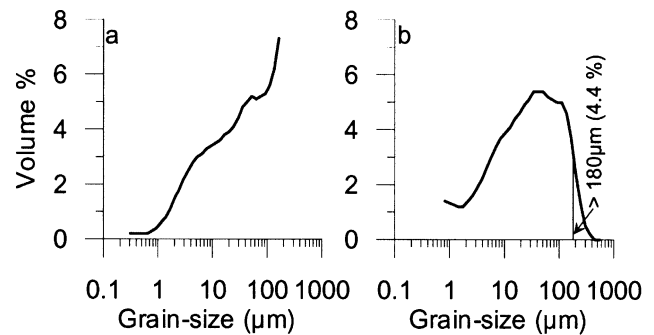


Fig. 7. Examples of the influence of the presence of particles outside the size range of a laser diffraction instrument (Malvern MasterSizer/E). a) Sediment sample analysed with an optical configuration permitting size analysis in the range 0.5–180 µm, median diameter = 32 µm. b) The same sample analysed with an optical configuration of the laser permitting analysis in the size range 1.2–600 µm, median diameter = 30 µm. It is evident that just a small number of particles outside the size range (in this case about 5%) cause a rising "tail" in the size spectrum. However, the influence of particles outside the size range on the median diameter is limited.

180 µm. More important, the D_{50} in Fig. 7a, b is, respectively, 31.8 and 30.2 µm. Thus, it may be concluded that the presence of particles outside of the measurement range of laser sizers causes a visible change in the size spectrum, but apparently no significant variation in the D_{50} .

The overall variation in W_{50} (0.03–2.6 mm s⁻¹) is realistic for coastal waters when compared to what is found in the literature. Alldredge and Gotschalk (1989) found individual floc settling velocities between 0.6 and 2.3 mm s⁻¹ for diatom flocs in the Southern California Bight and California Current. Millward et al. (1999) found median settling velocities between 0.001 and 0.2 mm s⁻¹ for suspended matter in the Humber Estuary and the coastal waters off the Holderness, NE-England. Dyer et al. (1996) reports a range in measured values of W_{50} from 0.0003 to 5 mm s⁻¹ for samples obtained with various kinds of instruments in the Elbe Estuary, Germany. Finally, ten Brinke (1997) reports on W_{50} varying between 0.6 and 2.4 mm s⁻¹ in the Oosterschelde tidal waters, the Netherlands. Summing up, the values for W_{50} found in this study (obtained using the method described by Mikkelsen and Pejrup, 2001) are all found to be within the range of values reported in the literature for similar waters.

Investigating the relationship between *c* vs *TSM*, *VC* vs *TSM* and *TSM* vs *PSA* (Fig. 8), it is found that there is no significant ($P > 0.01$) correlation. This demonstrates that a large variation in the size and density of the suspended aggregates exists (cf. Mikkelsen, 2001). A highly significant ($P < 0.01$) correlation between *c* and *PSA* is found. This is in accordance with optics theory, which states that the beam attenuation is proportional with the cross-sectional surface area of the particles (van de Hulst, 1957).

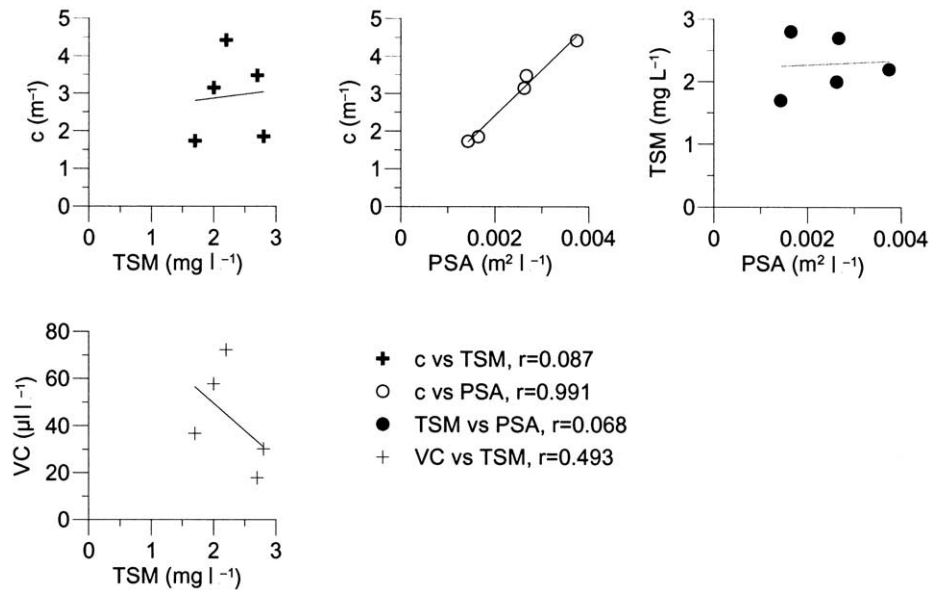


Fig. 8. Relationships between area-averaged values of c , TSM , PSA and VC (cf. Table 1). Only the relationship between c and PSA is significant ($P < 0.01$).

4. Conclusion

A LISST-100 in situ laser particle diffraction sizer was used to measure the spatial and temporal variation of a number of particle characteristics in two Danish coastal water-bodies: at an exposed site in the North Sea off the Danish west coast and in a sheltered fjord, the Horsens Fjord, on the east coast of the Jutland peninsula. Measurements were carried out at both sites in June and September of 1999. Prior to field work in June weather had been calm, while in September windy conditions had prevailed.

Area-averaged concentrations of total suspended matter concentration (TSM) increased from June to September at both sites, up to a factor of 1.5 while at the same time there was a decrease in particle size related parameters such as in situ median aggregate diameter (changed by a factor of up to 8), in situ effective density (by a factor of up to 5), in situ settling velocity (by a factor of up to 15), and in situ vertical particle flux (by a factor of up to 10).

It is suggested that because of an increase in wave- and wind-induced turbulence due to the windy conditions in September at the North Sea site, the observed changes are related to resuspension of bottom sediments (increasing TSM) and turbulence induced aggregate break-up. This is supported by changes in the fractal dimension, which is observed to increase for both sites from June to September.

As the Horsens Fjord site is very sheltered, it is suggested that the observed changes in TSM between June and September are not related to resuspension. Rather, they are due to the fact that in September an algae bloom was in progress (as revealed by chl a measurements). The decreasing in situ median diameter, in situ settling velocity, and in situ vertical particle flux is probably related to biologically induced particle aggregation in the upper part of the water column. It is suggested that this caused the coarser aggre-

gates to settle out of the upper part of the water column, leaving finer aggregates behind. This is somewhat confirmed by a coarsening of the in situ particle sizes when going from the surface ($D_{50} \sim 20 \mu\text{m}$) towards the bottom ($D_{50} \sim 100\text{--}400 \mu\text{m}$).

A large variation in time and space of the in situ aggregate sizes, densities and settling velocities is documented, and there seems to be no such thing as a constant in situ particle size, density or settling velocity, at least not with respect to aggregated particles. This is supported by observed relationships between beam attenuation, TSM , volume concentration and particle surface area. Only the relationship between beam attenuation and particle surface area proved significant ($P < 0.01$). This demonstrates that large changes in aggregate size and density have taken place. Otherwise the relationships between beam attenuation and TSM , between beam attenuation and VC and between TSM and particle surface area would be significant (cf. Mikkelsen, 2002).

Acknowledgements

The fieldwork was carried out as part of the Deco project (Danish Environmental Monitoring of Coastal Waters) financed by grant no. 9600667 from the Danish Space Board, the Danish Natural Science Research Council, the Danish Technical Research Council and the Danish Agricultural and Veterinary Research Council. Skipper Henning Svinth on “*RV Grådyb*”, and skipper Torben Vang on “*RV Tyra*” together with their crews, are thanked for their co-operation during the cruises. Thanks are also extended to the DECO partners at the National Environmental Research Institute in Roskilde for chl a measurements, and to Lotte Nyborg and Trine Nissen (Institute of Geography, University of Copen

hagen) for, respectively, help during the field work and for supplying data necessary for the construction of Fig. 7. The constructive comments of Dr. C.F. Jago and an anonymous reviewer were highly appreciated.

References

- Agrawal, Y.C., Pottsmith, H.C., 2000. Instruments for particle size and settling velocity observations in sediment transport. *Mar. Geol.* 168, 89–114.
- Aldredge, A.L., Gotschalk, C.C., 1989. Direct observations of the mass flocculation of diatom blooms: characteristics, settling velocities and formation of diatom aggregates. *Deep-Sea Res.* 36, 159–171.
- Andersen, T.J., 1999. Suspended sediment transport and sediment reworking at an intertidal mudflat, the Danish Wadden Sea. *Meddelelser fra Skalling-Laboratoriet XXXVII*, Institute of Geography, University of Copenhagen.
- Avnimelech, Y., Troeger, B.W., Reed, L.W., 1982. Mutual flocculation of algae and clay: Evidence and implications. *Science* 216, 63–65.
- Baban, S.M.J., 1993. Detecting water quality parameters in the Norfolk Broads, U.K., using Landsat imagery. *Int. J. Remote Sens.* 14, 1247–1267.
- Baban, S.M.J., 1997. Environmental monitoring of estuaries; estimating and mapping various environmental indicators in Breydon Water Estuary, U.K., using Landsat TM imagery. *Estuar. Coast. Shelf Sci.* 44, 589–598.
- Bale, A.J., Tocher, M.D., Weaver, R., Hudson, S.J., Aiken, J., 1994. Laboratory measurements of the spectral properties of estuarine suspended particles. *Neth. J. Aquat. Ecol.* 28, 237–244.
- Dyer, K.R., Cornelisse, J., Dearnaley, M.P., Fennessy, M.J., Jones, S.E., Kappenberg, J., McCave, I.N., Pejrup, M., Puls, W., van Leussen, W., Wolfstein, K., 1996. A comparison of in situ techniques for estuarine floc settling velocity measurements. *J. Sea Res.* 36, 15–29.
- Eisma, D., 1986. Flocculation and de-flocculation of suspended matter in estuaries. *Neth. J. Sea Res.* 20, 183–199.
- Forget, P., Ouillon, S., Lahet, F., Broche, P., 1999. Inversion of reflectance spectra of nonchlorophyllous turbid coastal waters. *Remote Sens. Environ.* 68, 264–272.
- Holdaway, G.P., Thorne, P.D., Flatt, D., Jones, S.E., Prandle, D., 1999. Comparison between ADCP and transmissometer measurements of suspended sediment concentration. *Cont. Shelf Res.* 19, 421–441.
- Kranenburg, C., 1994. The fractal structure of cohesive sediment aggregates. *Estuar. Coast. Shelf Sci.* 39, 451–460.
- Mari, X., Kjørboe, T., 1996. Abundance, size distribution and bacterial colonization of transparent exopolymeric particles (TEP) during spring in the Kattegat. *J. Plankton Res.* 18, 969–986.
- Mikkelsen, O.A., in press. Variation in the projected surface area of suspended particles: Implications for remote sensing assessment of TSM. *Remote Sens. Environ.* 79, 23–29.
- Mikkelsen, O.A., Pejrup, M., 2000. In situ particle size spectra and density of particle aggregates in a dredging plume. *Mar. Geol.* 170, 443–459.
- Mikkelsen, O.A., Pejrup, M., 2001. The use of a LISST-100 laser particle sizer for in situ estimates of floc size, density and settling velocity. *Geo-Mar. Lett.* 20, 187–195 DOI, 10.1007/s003670100064.
- Millward, G.E., Sands, T.K., Jago, C.F., 1999. Particulate metals and their settling velocities in the Humber Estuary. *UK. Mar. Chem.* 68, 145–168.
- Passow, U., Shipe, R.F., Murray, A., Pak, D.K., Brzezinski, M.A., Aldredge, A.L., 2001. The origin of transparent exopolymer particles (TEP) and their role in the sedimentation of particulate matter. *Cont. Shelf Res.* 21, 327–346.
- Risović, D., 1998. On correlation of fractal dimensions of marine particles with depth. *J. Colloid. Interf. Sci.* 197, 391–394.
- Ritchie, J.C., Cooper, C.M., 1988. Comparison of measured suspended sediment concentrations with suspended sediment concentrations estimated from Landsat MSS data. *Int. J. Remote Sens.* 9, 379–387.
- Robinson, M.C., Morris, K.P., Dyer, K.R., 1998. Deriving fluxes of suspended particulate matter in the Humber Estuary, UK, using airborne remote sensing. *Mar. Poll. Bull.* 37, 155–163.
- Sternberg, R.W., Berhane, I., Ogston, A.S., 1999. Measurement of size and settling velocity of suspended aggregates on the northern California continental shelf. *Mar. Geol.* 154, 43–53.
- Stumpf, R.P., Goldschmidt, P.M., 1992. Remote sensing of suspended sediment discharge into the western Gulf of Maine during the April 1987 100-year flood. *J. Coastal Res.* 8, 218–225.
- ten Brinke, W.B.M., 1997. Temporal variability in aggregate size and settling velocity in the Oosterschelde (The Netherlands). In: Burt, N., Parker, R., Watts, J. (Eds.), *Cohesive Sediments*. John Wiley & Sons, pp. 63–73.
- van de Hulst, H.C., 1957. *Light scattering by small particles*. John Wiley & Sons, New York, NY, USA.
- van der Lee, W.T.B., 2000. The settling of mud flocs in the Dollard estuary, The Netherlands. *Neth. Geogr. Stud.* 274. Ph.D. thesis. University of Utrecht, Utrecht, the Netherlands.